**SUPPLEMENTARY INFORMATION**

**Myocardial infarction accelerates atherosclerosis**

Partha Dutta et al.

Corresponding authors: Matthias Nahrendorf, Filip K. Swirski, Ralph Weissleder
Center for Systems Biology
185 Cambridge Street
Boston, MA 02114
Tel: (617) 643-0500
Fax: (617) 643-6133
mnahrendorf@mgh.harvard.edu
fswirski@mgh.harvard.edu
rweissleder@mgh.harvard.edu

**SUPPLEMENTARY FIGURES**
**Supplementary Figure 1**

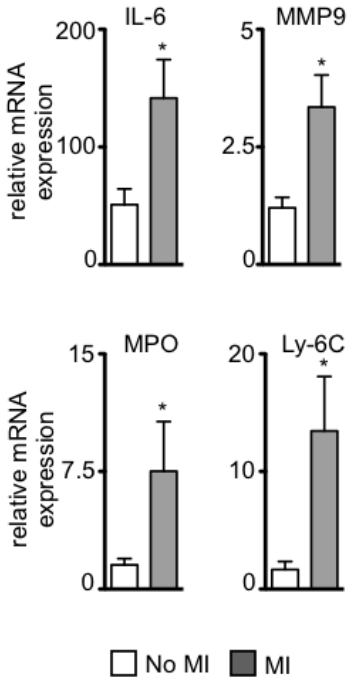


**Supplementary Figure 1: MI increases inflammatory gene expression in atherosclerotic plaques.**
Bar graphs show qPCR of aortic roots excised from apoE$^{-/-}$ mice with and without coronary ligation (n = 5 per group, 3 weeks after MI). mRNA levels were normalized to Gapdh Ct values. Mean ± s.e.m., * $P < 0.05$.

**Supplementary Figure 2**

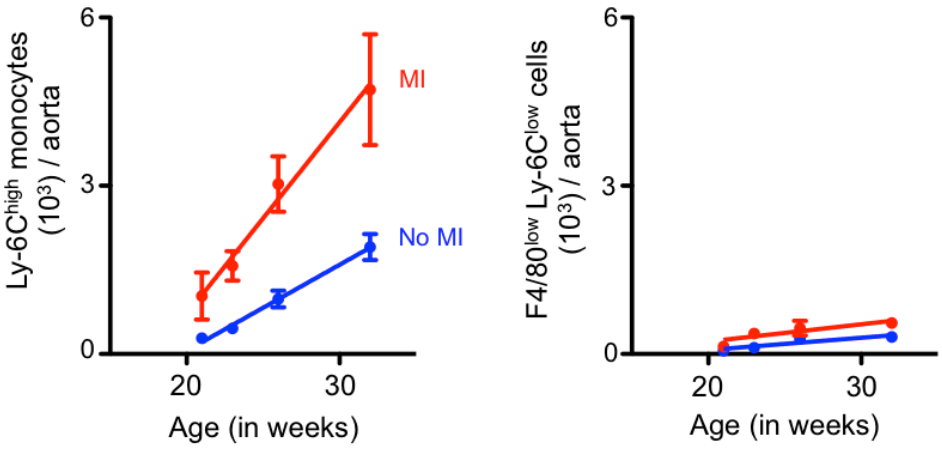


**Supplementary Figure 2: Fitting Ly-6C$^{high}$ monocyte content in the plaque as a function of age.**

Myocardial infarction, induced at 20 weeks of age, significantly accelerated accumulation of inflammatory monocytes in atherosclerotic plaque. The graph shows means for apoE$^{-/-}$ mice that received MI (red) or not (blue). The lines represent the linear fit of data from respective groups (n = 30 per group). The slopes of the lines were significantly different (p = 0.037). The goodness of fit ($R^2$) was 0.78 and 0.75, respectively. The right panel shows the increase of F4/80$^{low}$ Ly-6C$^{low}$ cells in aortae. Here, the slope did not differ significantly between infarct and control cohorts.

**Supplementary Figure 3**

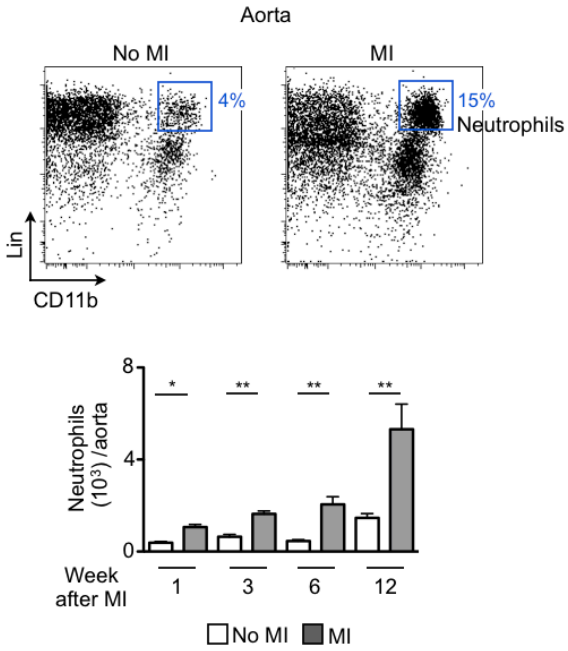


**Supplementary Figure 3: Neutrophil levels in atherosclerotic plaque after MI.**
Quantification of neutrophils (lineage$^+$ CD11b$^+$ cells) in atherosclerotic plaques at different time points after MI. Age matched apoE$^{-/-}$ mice without MI served as controls (n = 5–9 per group). Representative dot plots from the experiment at 3 weeks after MI are shown. Mean ± s.e.m., * $P < 0.05$, ** $P < 0.01$.

**Supplementary Figure 4**

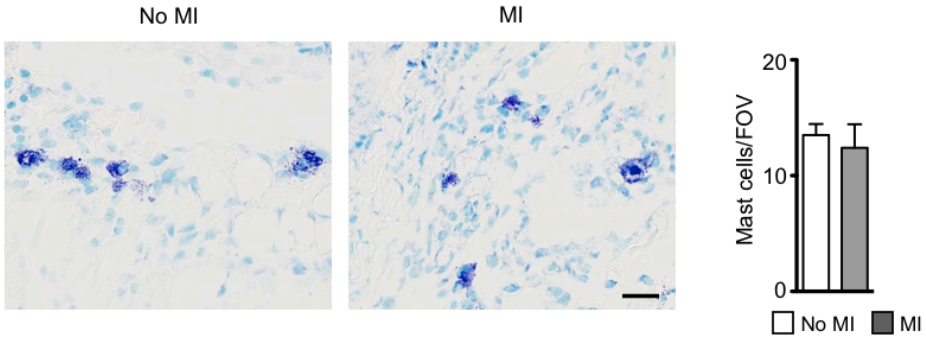


**Supplementary Figure 4: Mast cell levels in aorta after MI.**
Aortic root sections were stained with toluidine blue to detect mast cells (n = 7–9 per group). Scale bar indicates 25 μm. Mean ± s.e.m.

**Supplementary Figure 5**

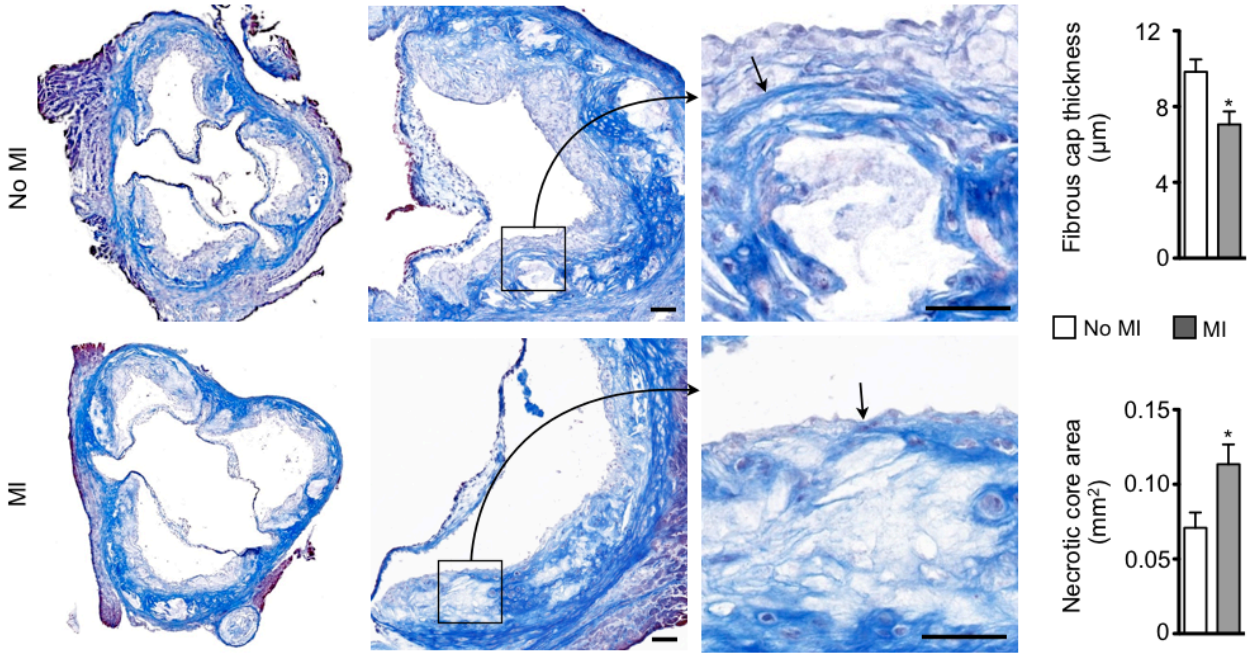


**Supplementary Figure 5: Fibrous cap thickness and necrotic core area in plaque after MI.** Masson staining on aortic roots harvested from apoE$^{-/-}$ mice 3 weeks after MI and age-matched control apoE$^{-/-}$ mice (n = 7–11 per group). Scale bar indicates 50 µm, arrows point at fibrous cap above necrotic core. Bar graphs show fibrous cap thickness and necrotic core area per section. Mean ± s.e.m., * $P < 0.05$.

**Supplementary Figure 6**

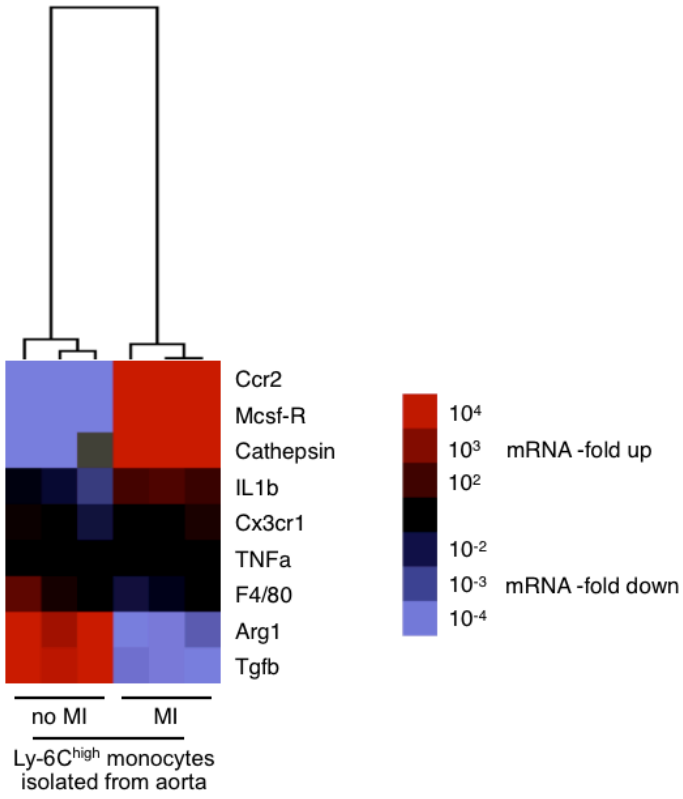


**Supplementary Figure 6: Plaque monocytes express higher levels of inflammatory genes after MI.**

Ly-6C$^{high}$ monocytes were isolated from aortae by flow sorting and then analyzed by qPCR (n = 3 apoE$^{-/-}$ mice per group, MI: 3 weeks after coronary ligation).

**Supplementary Figure 7**

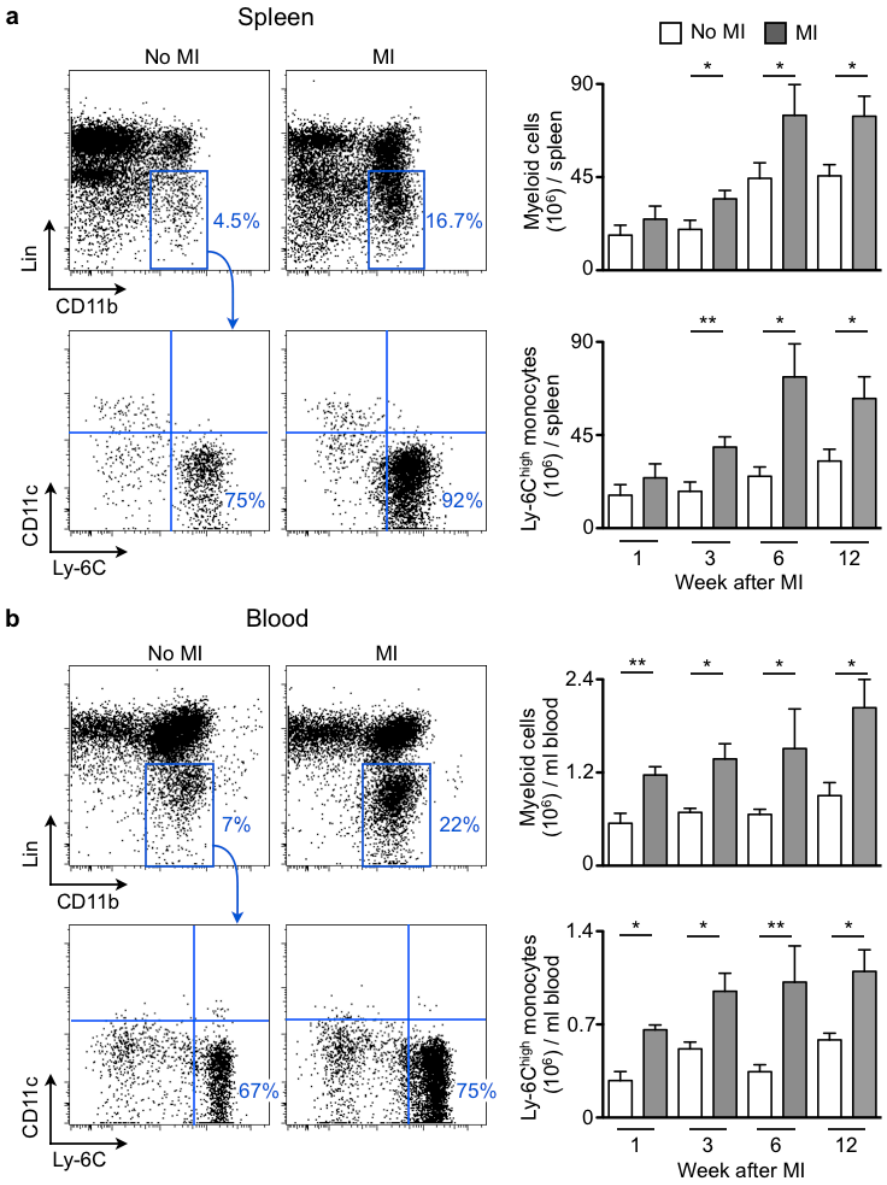


**Supplementary Figure 7: Monocytosis in the spleen and blood after MI.**
FACS quantification of myeloid cells and Ly-6C$^{high}$ monocytes in the spleen (**a**) and blood (**b**) of apoE$^{-/-}$ mice at different time points after MI (n = 3–9 per group). Blue rectangular gates show myeloid cells and lower right quadrants show Ly-6C$^{high}$ monocytes. Age matched apoE$^{-/-}$ mice without MI served as controls. Mean ± s.e.m., * $P < 0.05$, ** $P < 0.01$.

**Supplementary Figure 8**

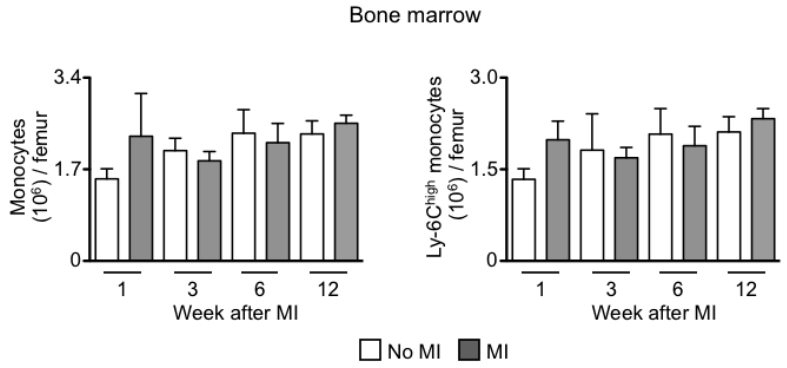


**Supplementary Figure 8: Monocyte levels in the bone marrow.**
Levels of total monocytes (left) and Ly-6C$^{high}$ monocytes in the bone marrow at different time points after MI were measured by flow cytometry (n = 3–9 per group). Age-matched apoE$^{-/-}$ mice without MI were used as control (No MI). Mean ± s.e.m.

**Supplementary Figure 9**

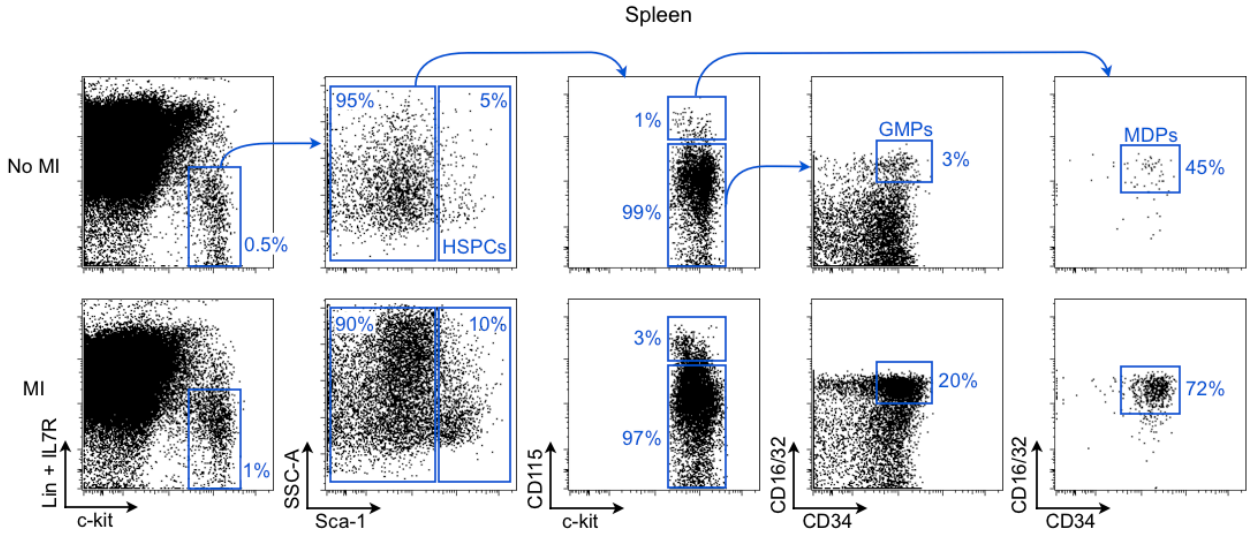


**Supplementary Figure 9: Flow cytometric gating strategy for progenitor cells.**
Flow cytometric gating for HSPCs, MDPs, and GMPs in the spleen of apoE$^{-/-}$ mice with and without MI. Hematopoietic stem and progenitors cells (HSPCs) were identified as lineage (CD90/B220/CD49b/NK1.1/Ly-6G/Ter119/CD11b/CD11c/IL7Rα)$^{low}$ c-kit$^{high}$ Sca-1$^{high}$. Granulocyte and macrophage progenitors (GMPs) were identified as lineage$^{low}$ c-kit$^{high}$ Sca-1$^{low}$ CD115$^{low}$ CD16/32$^{high}$ CD34$^{high}$. Macrophage dendritic cell progenitors (MDPs) were identified as lineage$^{low}$ c-kit$^{high}$ Sca-1$^{low}$ CD115$^{high}$ CD16/32$^{high}$ CD34$^{high}$. Absolute numbers of progenitors in spleen are shown in Fig. 2.

**Supplementary Figure 10**

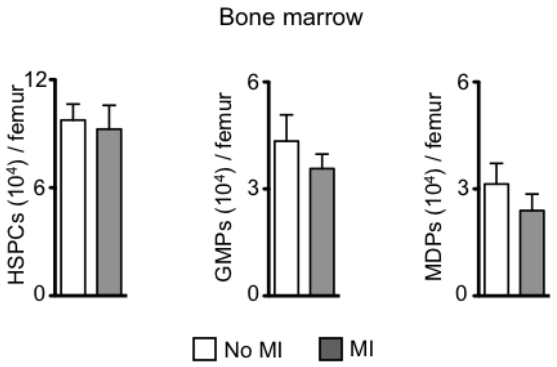


**Supplementary Figure 10: Progenitor cell numbers in the bone marrow.**
Levels of HSPCs, GMPs and MDPs in the bone marrow of apoE$^{-/-}$ mice were unchanged 3 weeks after MI (n = 12–15 per group). Mean ± s.e.m.

**Supplementary Figure 11**

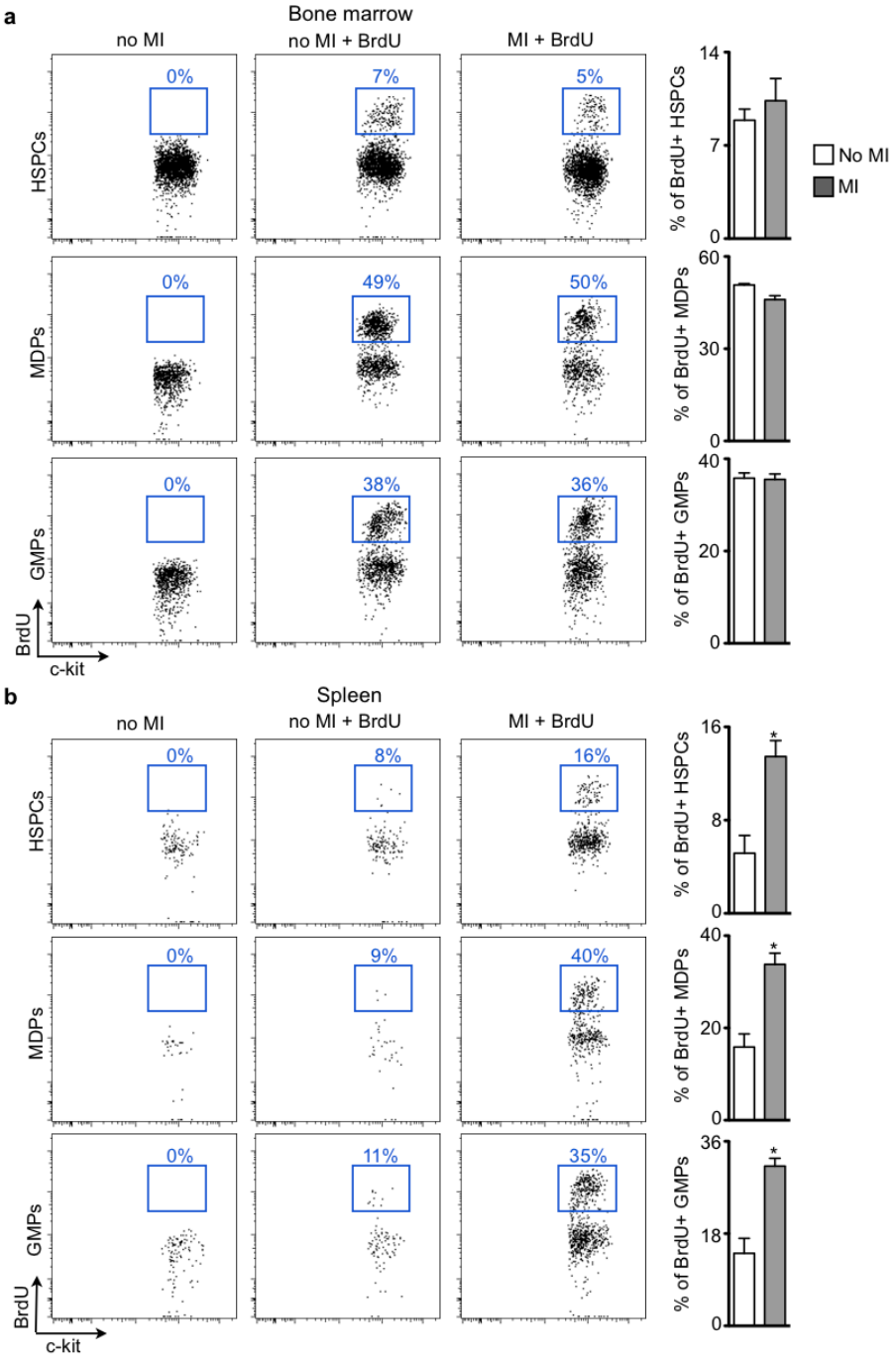


**Supplementary Figure 11: Splenic progenitor proliferation after MI.**
Proliferation of progenitor cells in C57BL/6 mice was measured by in vivo BrdU incorporation assay. BrdU was injected intraperitoneally on day 3 after MI and BrdU$^+$ HSPCs, GMPs and MDPs in the bone marrow (**a**) and spleen (**b**) were quantified by flow cytometry on day 4 after MI. Naive C57BL/6 mice without MI injected or not injected with BrdU served as controls (n = 4–5 per group). Mean ± s.e.m., * $P < 0.05$.

**Supplementary Figure 12**

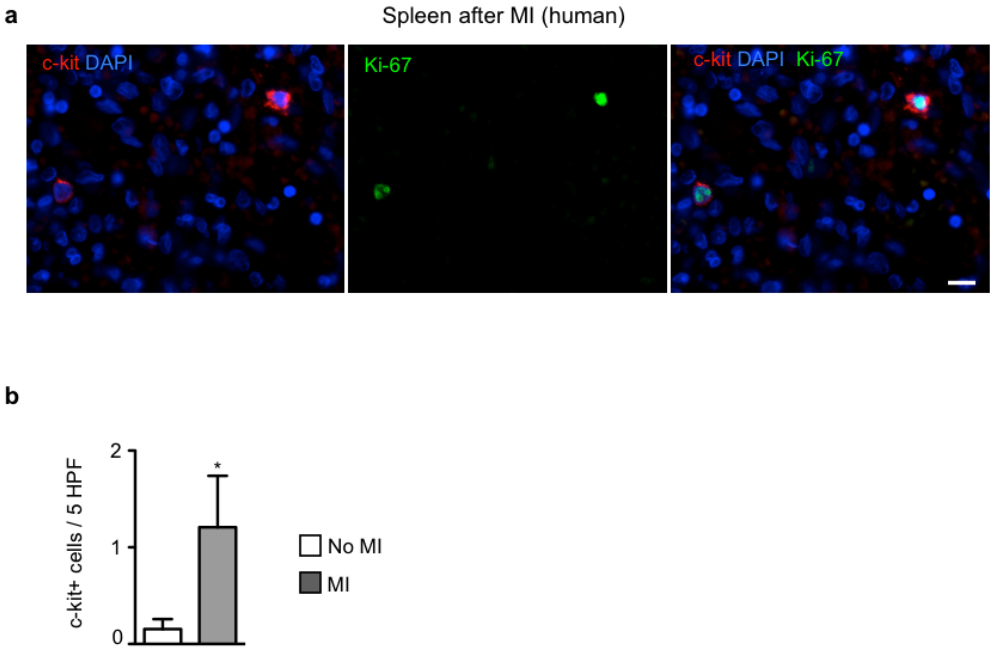


**Supplementary Figure 12: Splenic progenitors in patients with MI.**
**a,** Immunoreactive staining for c-kit and Ki-67 in a patient with subacute MI. Scale bar indicates 14 μm. **b**, Enumeration of c-kit$^{+}$ mast cell tryptase$^{-}$ cells in the red pulp of the spleen in patients that died hours to days after myocardial infarction (MI, n = 29) or trauma control cases (No MI, n = 13). Mean ± s.e.m., * $P$ = 0.038 in one tailed Mann-Whitney test.

## Supplementary Figure 13

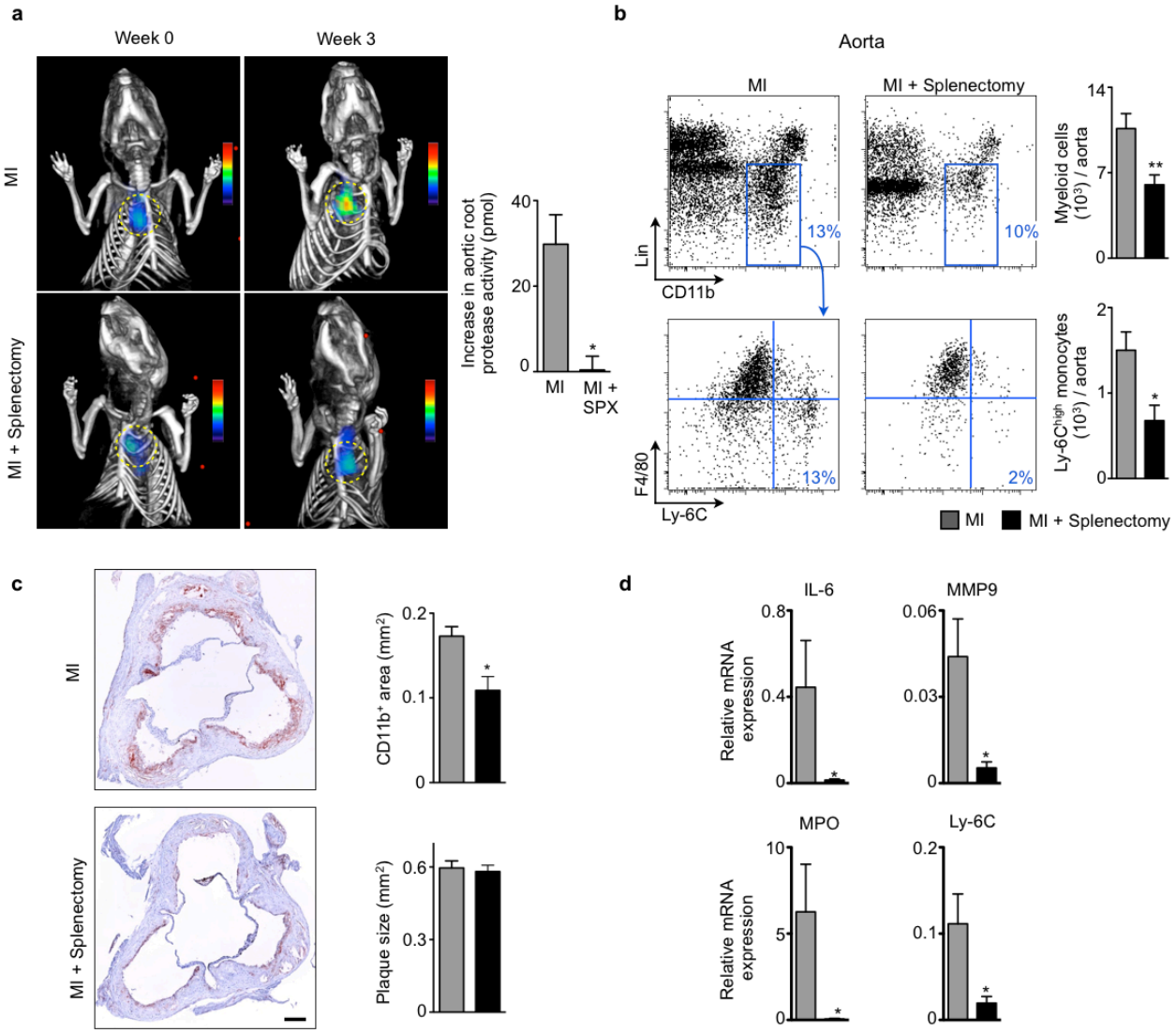


**Supplementary Figure 13: Splenic monocytes contribute to increased cell numbers in atherosclerotic plaque after MI.**

Splenectomy was performed in apoE$^{-/-}$ mice on the day of coronary ligation. **a,** Protease activity in aortic roots measured by FMT-CT before and then again 3 weeks after MI and splenectomy. Circles show aortic root area (n = 8–10 per group). **b,** Myeloid cells and Ly-6C$^{high}$ monocytes in the aorta were quantified and compared with apoE$^{-/-}$ mice with MI but without splenectomy (n = 6–12 per group). **c,** Immunohistochemical staining of aortic roots for CD11b (n = 10 per group). The scale bar represents 150 µm. **d,** qPCR analyses of aortic roots (n = 5 per group). Mean ± s.e.m., * $P < 0.05$, ** $P < 0.01$.

**Supplementary Figure 14**

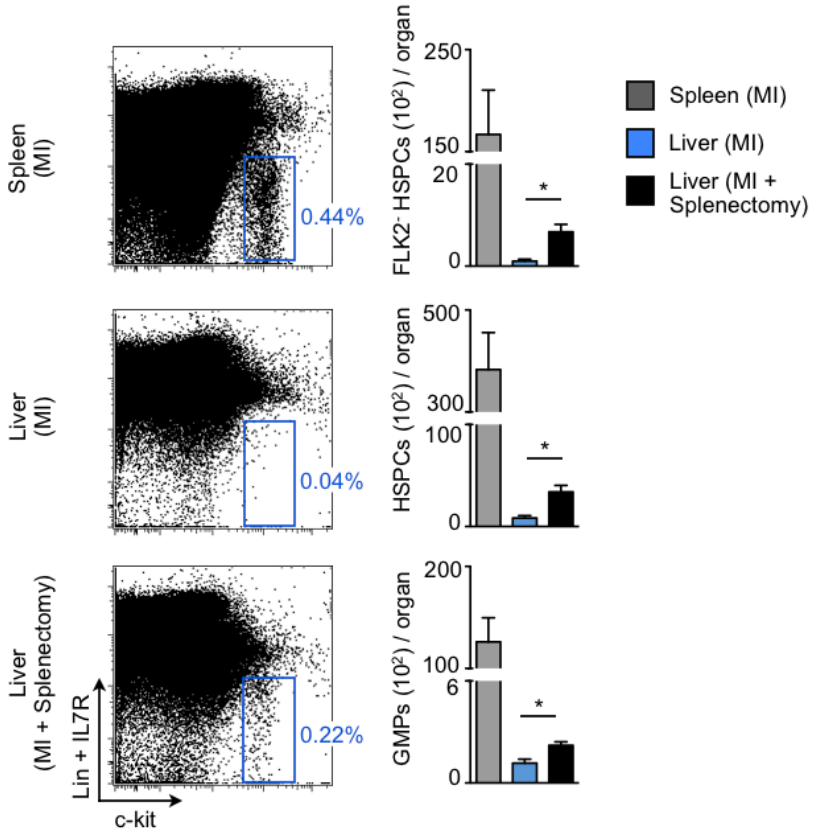


**Supplementary Figure 14: Progenitor cell levels in the liver after MI and splenectomy.** The liver can contribute to prenatal hematopoiesis; hence, we also investigated progenitors in this organ. Progenitor cell (Flk-2$^-$ HSPCs, HSPCs and GMPs) numbers in the liver and spleen of C57BL/6 mice were quantified using flow cytometry on day 4 after MI (with or without splenectomy) (n = 3–4 per group). Mean ± s.e.m., * $P < 0.05$.

**Supplementary Figure 15**

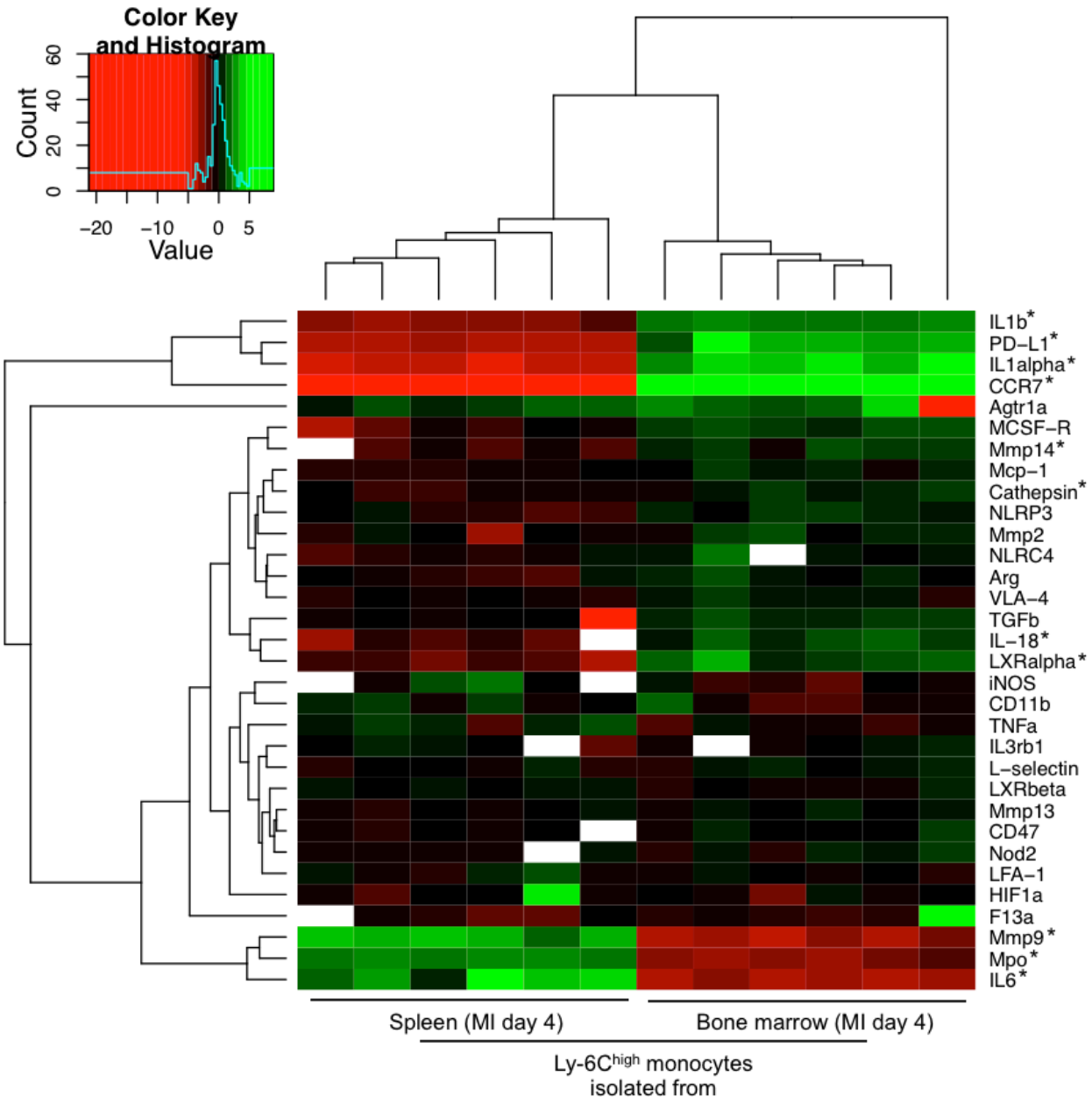


**Supplementary Figure 15: mRNA profile in splenic and bone marrow Ly-6C$^{high}$ monocytes after MI.**

Ly-6C$^{high}$ monocytes were sorted from the spleen and bone marrow on day 4 after coronary ligation in six C57BL/6 mice per group, a mRNA heat map is shown. * $P < 0.05$ ANOVA with Bonferroni post test comparing spleen versus bone marrow mRNA level.

## Supplementary Figure 16

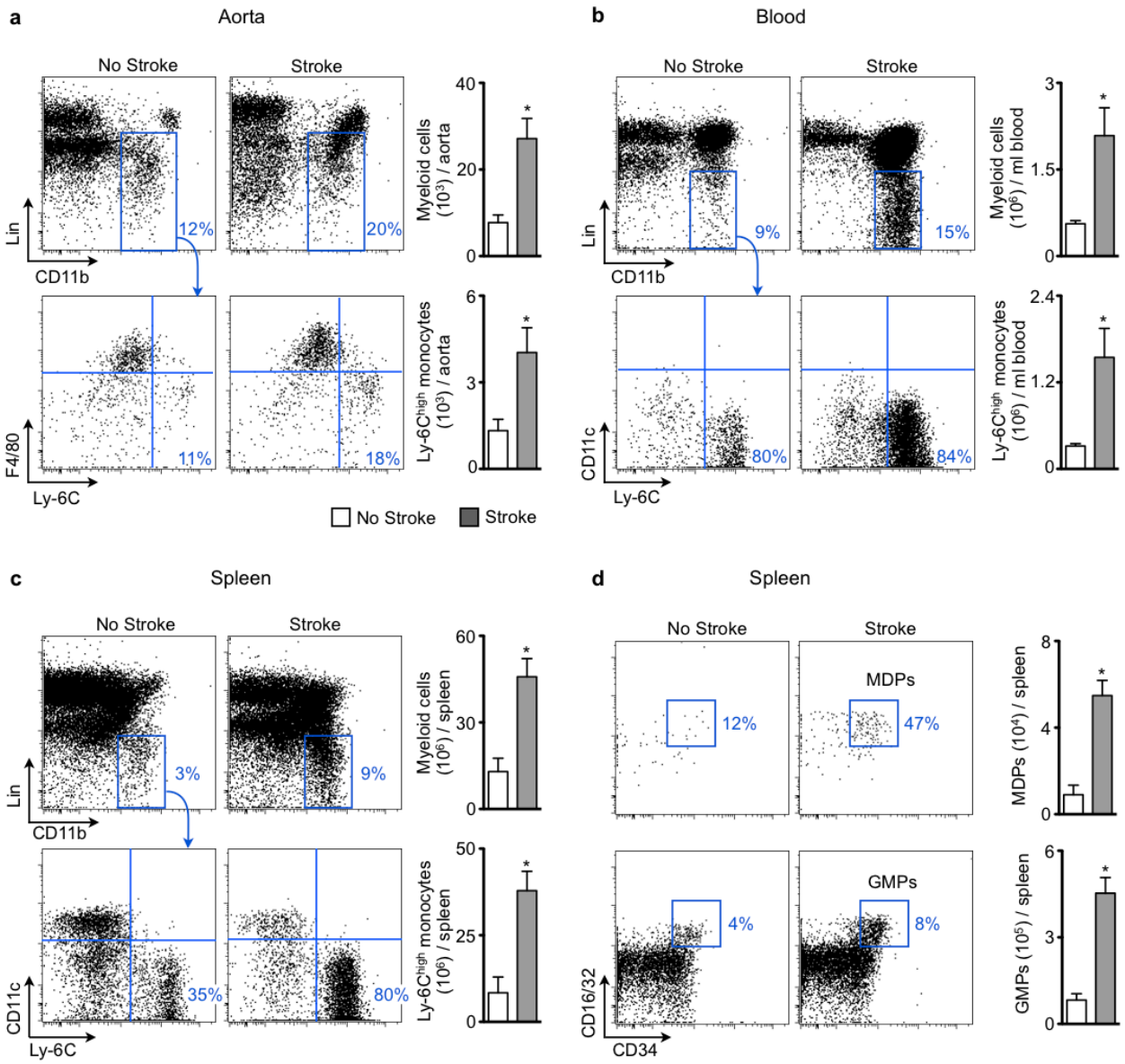


**Supplementary Figure 16: Stroke increases monocyte numbers in atherosclerotic plaque.** Organs were harvested 6 weeks after stroke in apoE$^{-/-}$ mice and analyzed by flow cytometry. Myeloid cells and Ly-6C$^{high}$ monocytes were quantified in the aorta (**a**), blood (**b**), and spleen (**c**). **d,** GMPs and MDPs in the spleen. ApoE$^{-/-}$ mice without stroke were used as control (n = 6–7 per group). Mean ± s.e.m., * $P < 0.05$, * $P < 0.01$.

**Supplementary Figure 17**

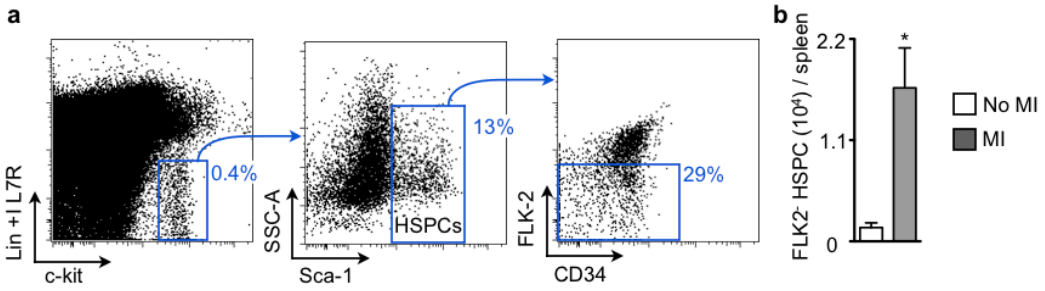


**Supplementary Figure 17: Flk-2$^-$ HSPCs in the spleen after MI.**
**a,** Gating strategy for Flk-2$^-$ HSPCs:CD90/B220/CD49b/NK1.1/Ly-6G/Ter119/CD11b/CD11c/IL7Rα)$^{low}$ c-kit$^{high}$ Sca-1$^{high}$ FLK-2$^{low}$ CD34$^{high/low}$ cells. b, Quantification of of Flk-2$^-$ HSPCs in the spleen 4 days after MI by flow cytometry (n = 3–6 per group). Mean ± s.e.m., * $P < 0.05$.

**Supplementary Figure 18**

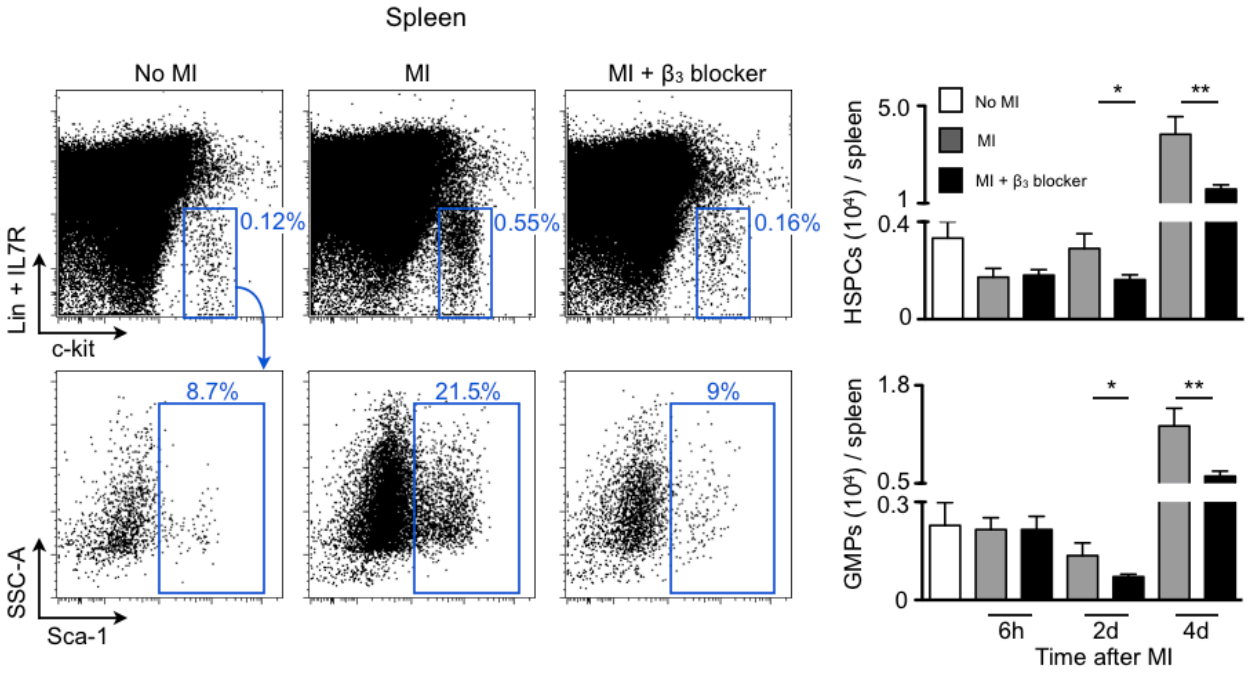


**Supplementary Figure 18: $\beta_3$ receptor antagonist treatment after MI reduces progenitor numbers in the spleen of wild type mice.**
C57BL/6 mice were treated with a $\beta_3$ receptor antagonist intraperitoneally twice daily after inducing MI. HSPCs and GMPs numbers in the spleen were analyzed by flow cytometry (n = 4–9 C57BL/6 mice per group). Mean ± s.e.m., * $P < 0.05$, ** $P < 0.01$.

**Supplementary Figure 19**

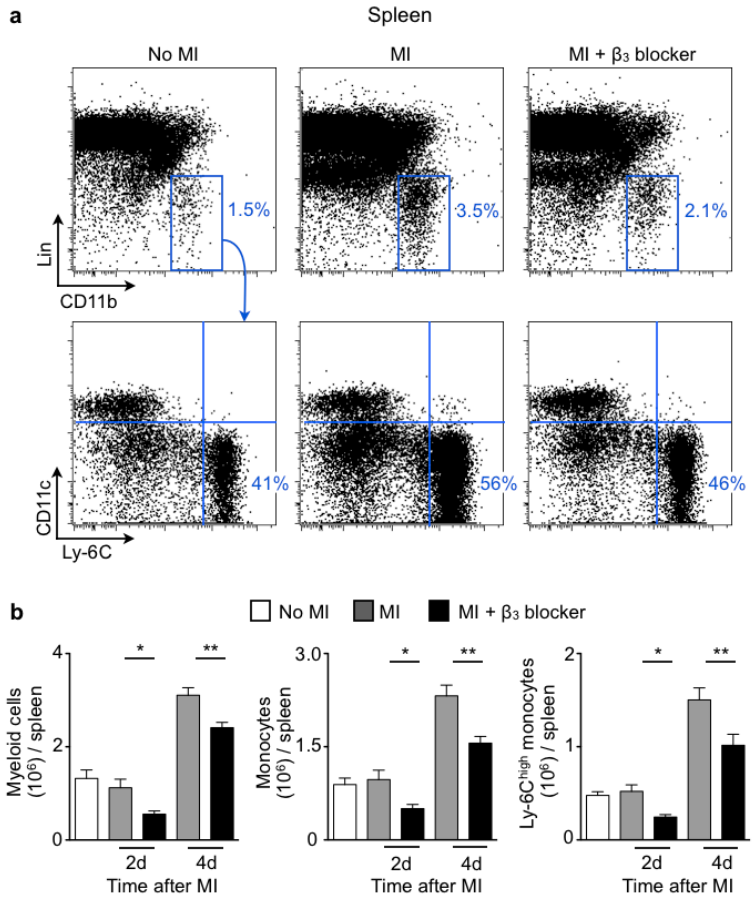


**Supplementary Figure 19: $\beta_3$ receptor antagonist treatment after MI reduces monocyte levels in the spleen of wild type mice.**
C57BL/6 mice were treated with a $\beta_3$ receptor antagonist intraperitoneally twice daily after inducing MI. **a,** Flow cytometric plots showing myeloid cells (blue gates in the upper panel) and Ly-6C$^{high}$ monocytes (lower right quadrant in the lower panel) in different treatment groups. **b,** Quantification of myeloid cells, monocytes, and Ly-6C$^{high}$ monocytes. Untreated mice with or without MI served as controls (n = 4–7 per group). Mean ± s.e.m., * $P < 0.05$, ** $P < 0.01$.

**Supplementary Figure 20**

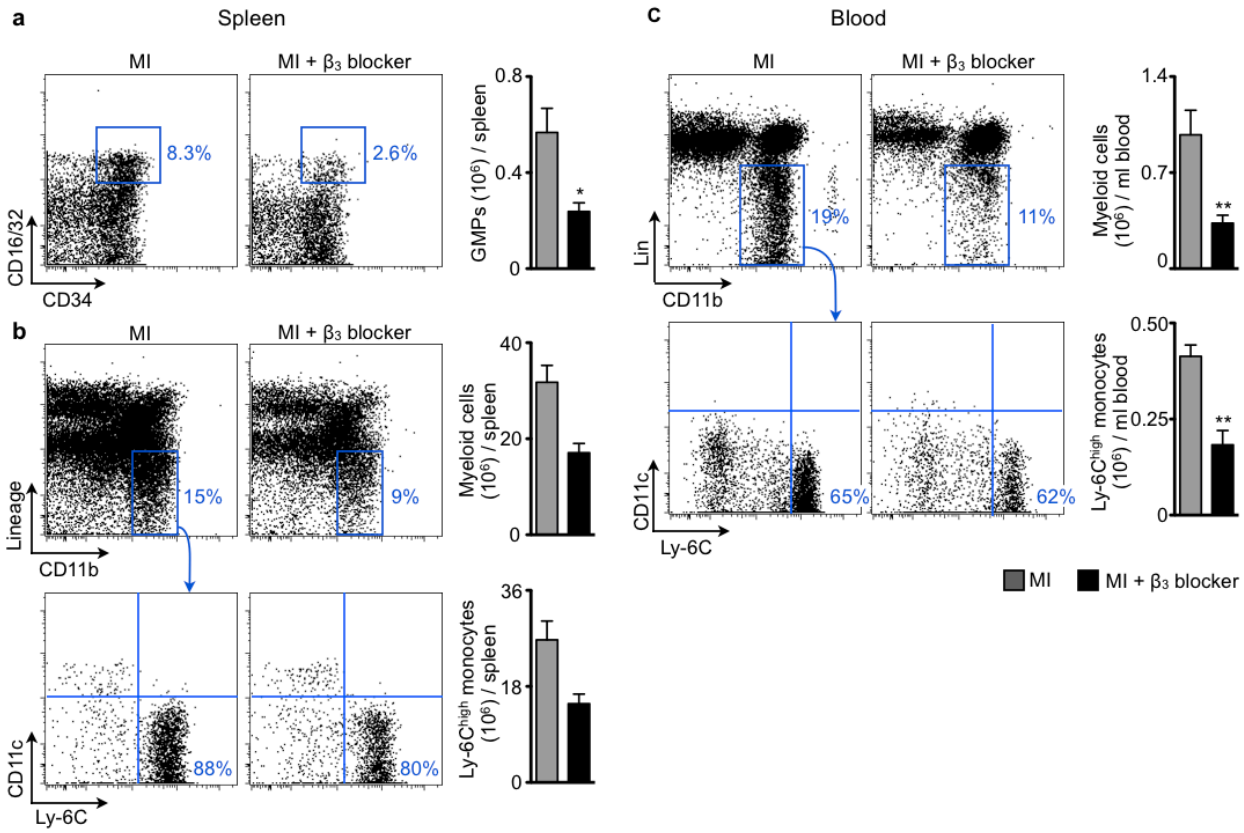


**Supplementary Figure 20: β3 receptor antagonist treatment after MI reduces monocyte and GMP levels in apoE$^{-/-}$ mice.**
ApoE$^{-/-}$ mice with MI were treated with a β3 receptor antagonist twice daily for three weeks (n = 6 per group). **a,** Flow cytometric plots showing GMPs (left) and quantification of GMPs (right) in the spleen. Their progeny, myeloid cells and Ly-6C$^{high}$ monocytes, were quantified in the spleen (**b**) and blood (**c**) and compared with untreated apoE$^{-/-}$ mice with MI. Mean ± s.e.m., * $P <$ 0.05, ** $P < 0.01$.

**Supplementary Figure 21**

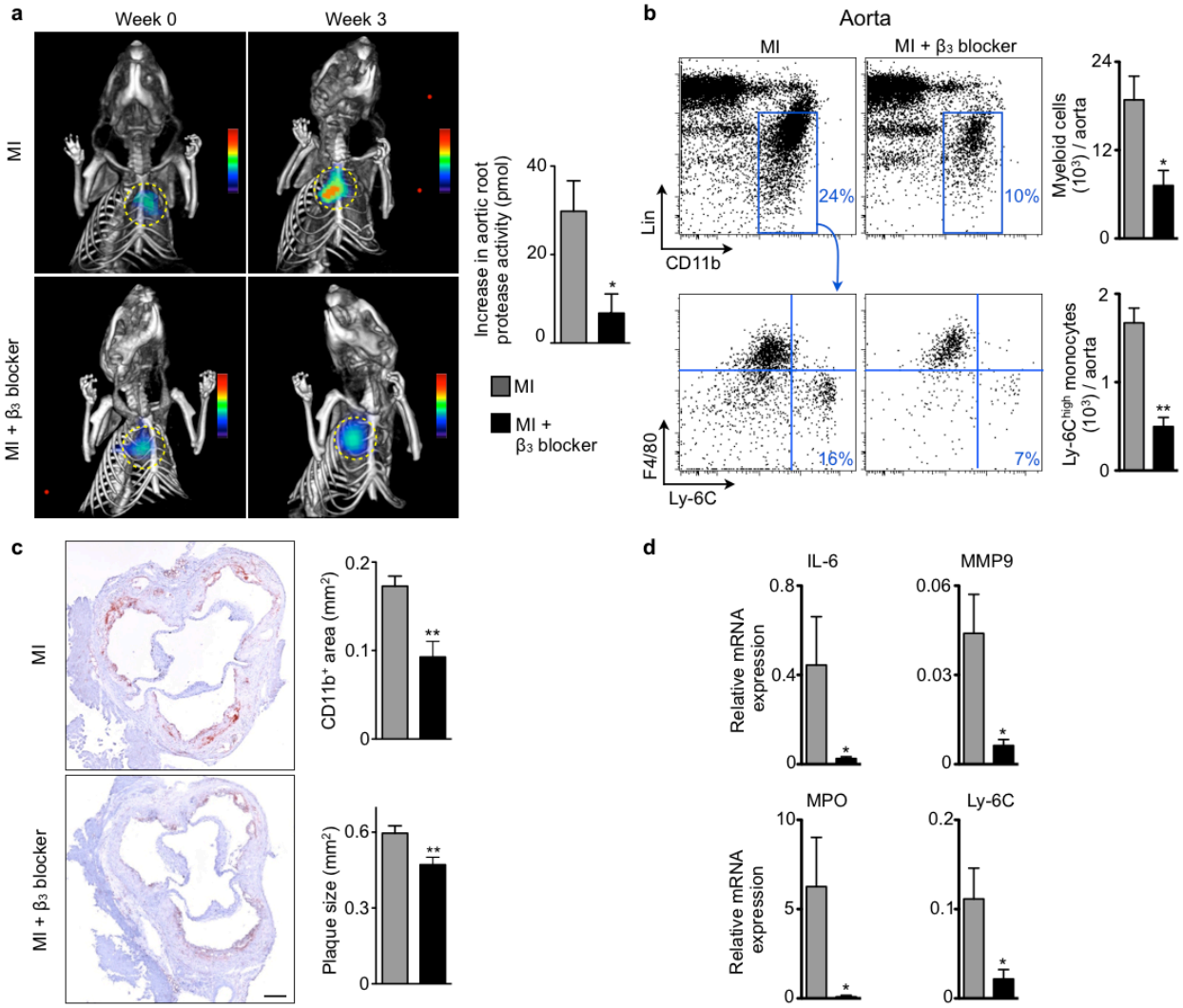


**Supplementary Figure 21: Treatment with a β3 receptor antagonist reduces atherosclerosis after MI.**

**a**, Protease activity in aortic roots measured by FMT-CT before and then again 3 weeks after MI. Circles show aortic root area (n = 8 per group). **b,** Flow cytometric plots showing myeloid cells (blue gates in the upper panel) and Ly-6C$^{high}$ monocytes (lower right quadrant in the lower panel) in apoE$^{-/-}$ mice 3 weeks after MI, treated with a β3 receptor antagonist (n = 6 per group). **c,** Immunohistochemical staining of aortic roots for CD11b after treatment with a β3 receptor antagonist (n = 10 per group). The scale bar represents 150 μm. **d**, qPCR analyses of aortic roots (n = 5 per group). Mean ± s.e.m., * $P < 0.05$, ** $P < 0.01$.

**Supplementary Figure 22**

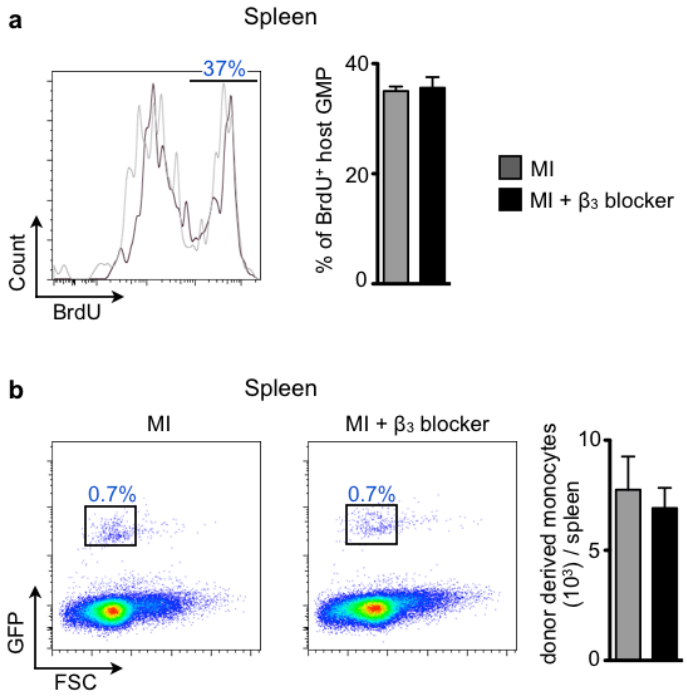


**Supplementary Figure 22: $\beta_3$ blocker treatment does not affect splenic monocyte differentiation.**
Flow cytometric analysis of splenocytes 4 days after MI in C57BL/6 mice treated or not treated with a $\beta_3$ blocker. **a,** Proliferation of host GMPs determined by BrdU incorporation (n = 5 per group). **b,** Quantification of $GFP^+$ monocytes 4 days after MI and adoptive transfer of $GFP^+$ GMPs (n = 5 per group).

**Supplementary Figure 23**

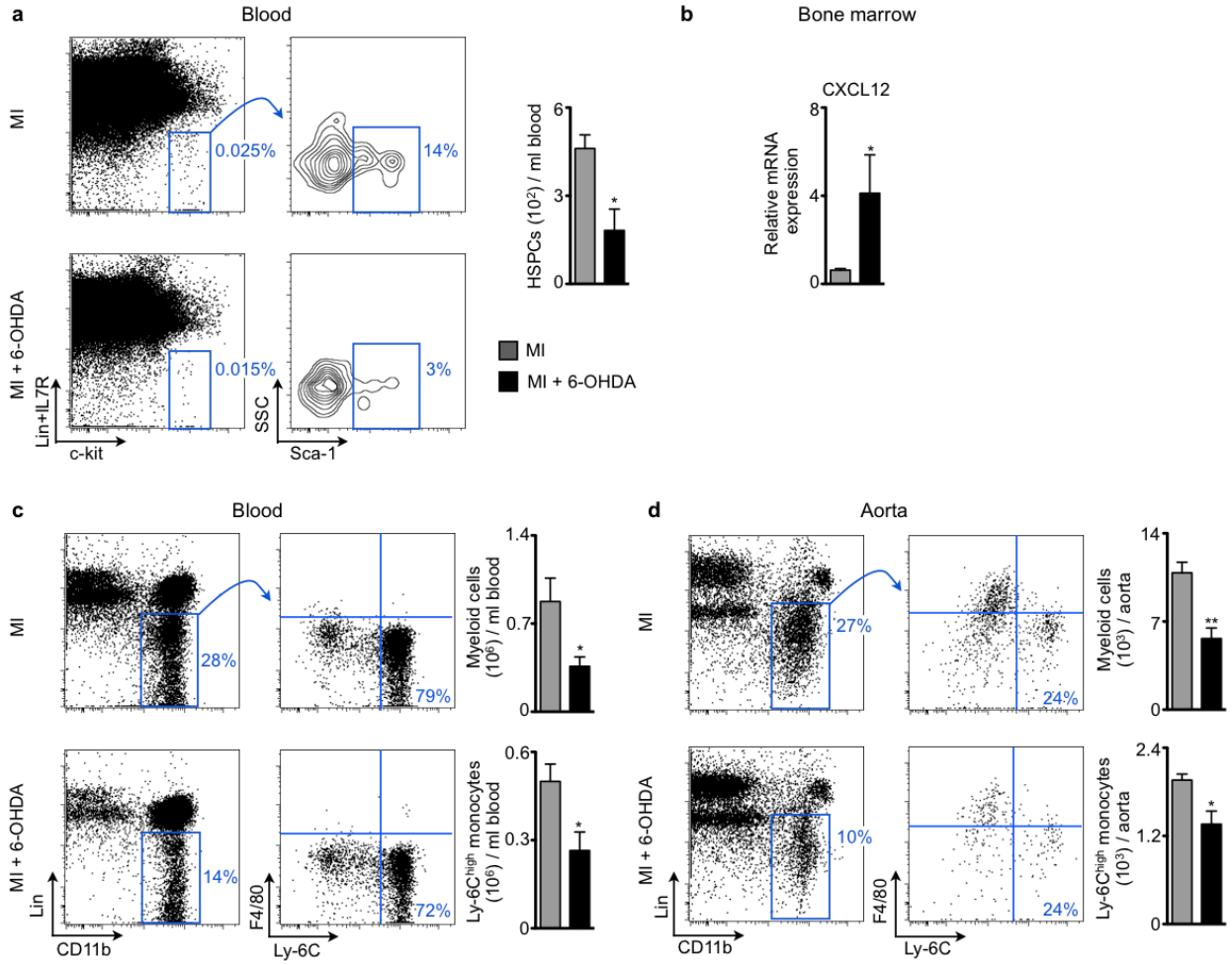


**Supplementary Figure 23: Chemical sympathectomy reduces atherosclerosis after MI.** **a,** Quantification of HSPCs 4 days after MI in blood of C57BL/6 mice treated or not treated with 6-OHDA (n = 5–16). **b,** mRNA level of CXCL12, an HSPC retention factor in the bone marrow of C57BL/6 mice with or without 6-OHDA treatment (n = 4–5 per group). Myeloid cells and Ly-6C$^{high}$ monocytes were quantified in blood (**c**) and the aortae (**d**) of apoE$^{-/-}$ mice treated or not treated with 6-OHDA for three weeks after MI (n = 5–7 per group). Mean ± s.e.m., * $P < 0.05$, ** $P < 0.01$.

**Supplementary Figure 24**

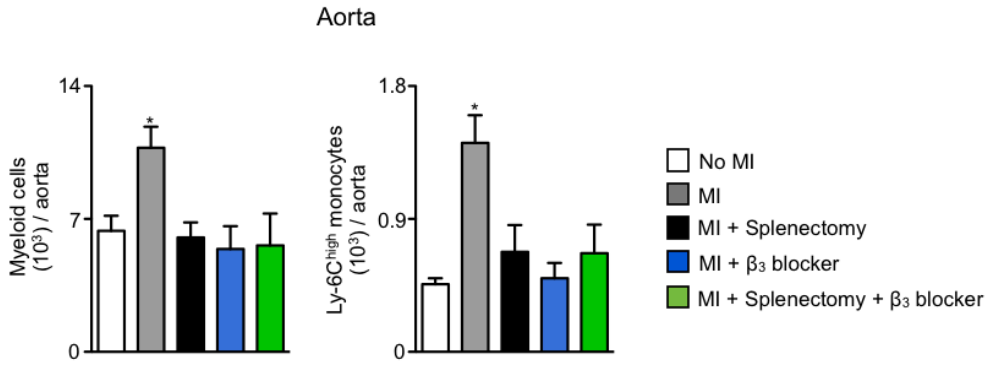


**Supplementary Figure 24: The effects of β3 blocker treatment with or without splenectomy on aortic myeloid cell content after MI.**
ApoE$^{-/-}$ mice received splenectomy on the day of MI, and 2 cohorts of apoE$^{-/-}$ mice were treated with a β3 blocker for three weeks. Myeloid cells and Ly-6C$^{high}$ monocytes were quantified in the aortae by flow cytometry. Age matched apoE$^{-/-}$ mice without MI served as control (n = 5–9 per group). Mean ± s.e.m., * $P < 0.05$ versus no MI, MI + splenectomy, and MI + β3 blocker treatment.

**Supplementary Figure 25**

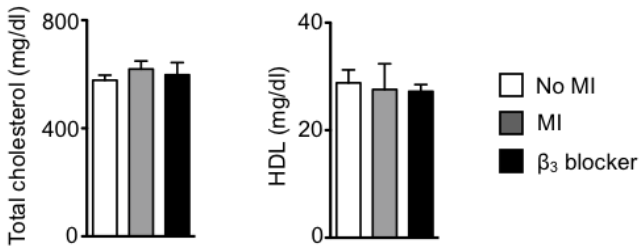


**Supplementary Figure 25: MI or treatment with a $\beta_3$ receptor antagonist does not change blood cholesterol and HDL levels.**
Serum was separated from blood drawn from apoE$^{-/-}$ mice that either received MI 3 weeks prior or were treated with a $\beta_3$ receptor antagonist twice daily for three weeks. Serum of naive apoE$^{-/-}$ mice was used as control. All groups received high cholesterol western type diet. Total cholesterol and HDL were measured in the serum using an enzymatic colorimetric assay (n = 11–12 per group).

**Supplementary Figure 26**

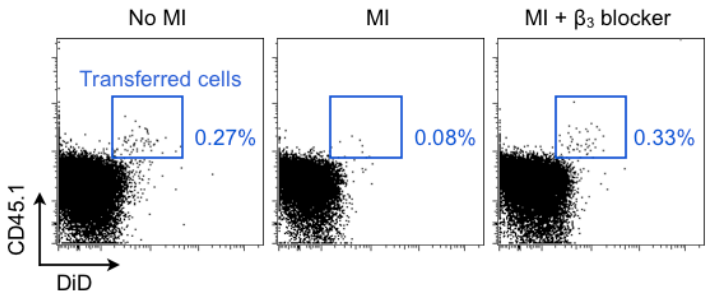


**Supplementary Figure 26: Release of DiD$^+$ HSPCs from the bone marrow after MI by flow cytometry.**
DiD labelled-HSPC cells assessed in the bone marrow by flow cytometry following intravital microscopy. Bone marrow cells were harvested, gated on Lin$^-$ IL7R$^-$ c-kit$^+$ Sca-1$^+$ cells. Blue gate shows adoptively transferred CD45.1$^+$ DiD$^+$ cells. These data confirm IVM results shown in Fig. 4.

**Supplementary Figure 27**

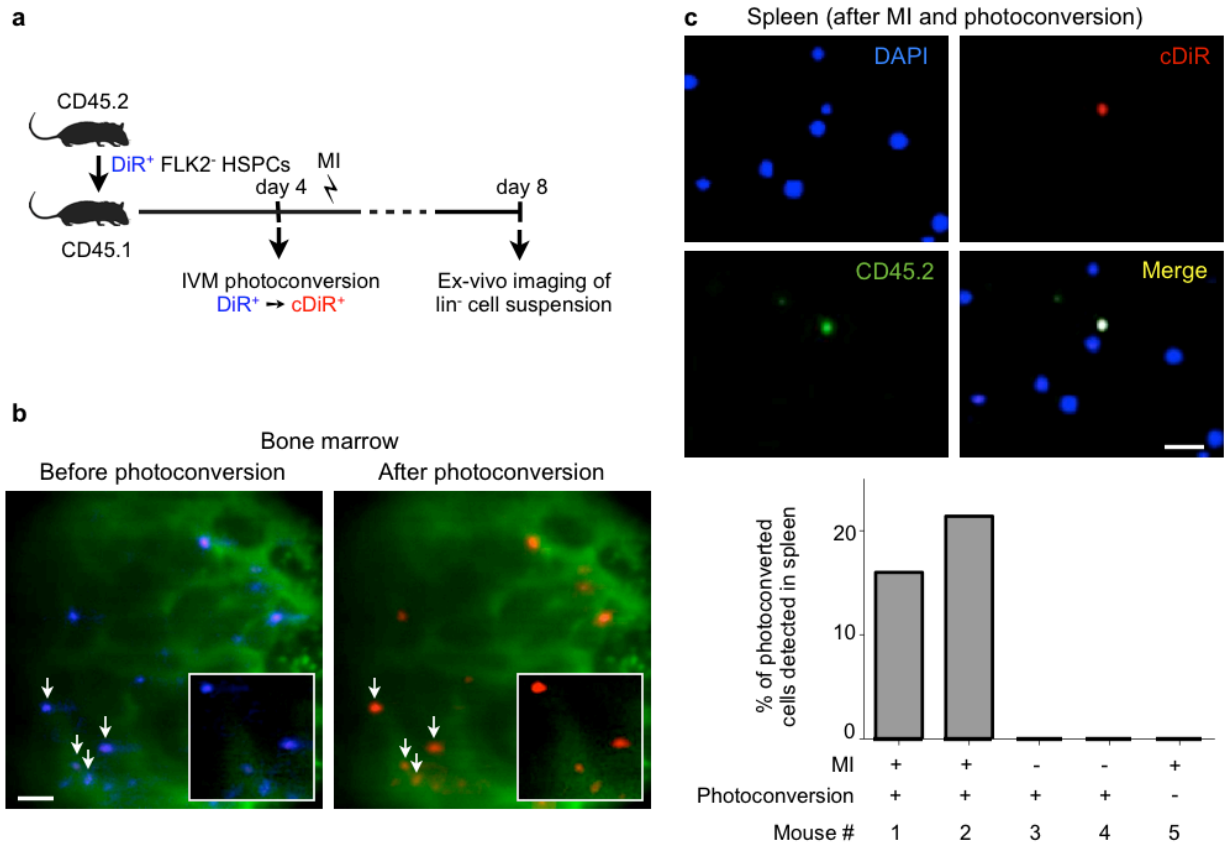


**Supplementary Figure 27: Bone marrow Flk-2$^-$ HSPCs relocate to the spleen after MI.** **a,** Experimental outline. **b,** DiR labelled HSPCs in the bone marrow by intravital microscopy (IVM) before (blue) and after photoconversion (red). The scale bar represents 50 µm, the inset is a higher magnification view of cells on the left (arrows). 18 ± 4 cells were photoconverted per mouse. **c,** Photoconverted cells were identified as cDIR$^+$DAPI$^+$CD45.2$^+$ in splenic cell suspensions 4 days after induction of MI by ex vivo imaging. The scale bar represents 20 µm. The bar graph depicts detected cells in the spleen as percentage of cells converted in the skull for individual cases.

**Supplementary Figure 28**

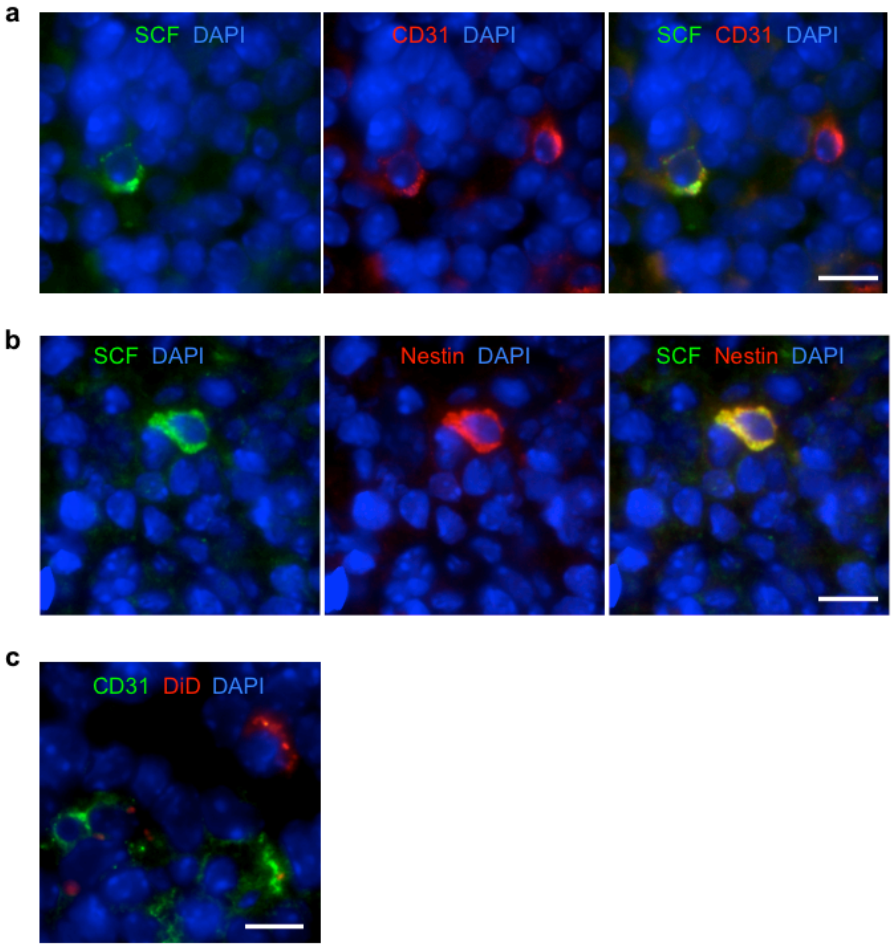


**Supplementary Figure 28: SCF-expressing cells in the spleen.**
Co-localization of SCF, CD31 and DAPI (**a**); and SCF, nestin and DAPI (**b**) by immunofluorescence microscopy of spleen sections 4 days after MI. **c,** Detection of adoptively transferred $DiD^+$ $Flk\text{-}2^-$ HSPCs in proximity to $CD31^+$ cells. Scale bar indicates 10 μm.

**Supplementary Figure 29**

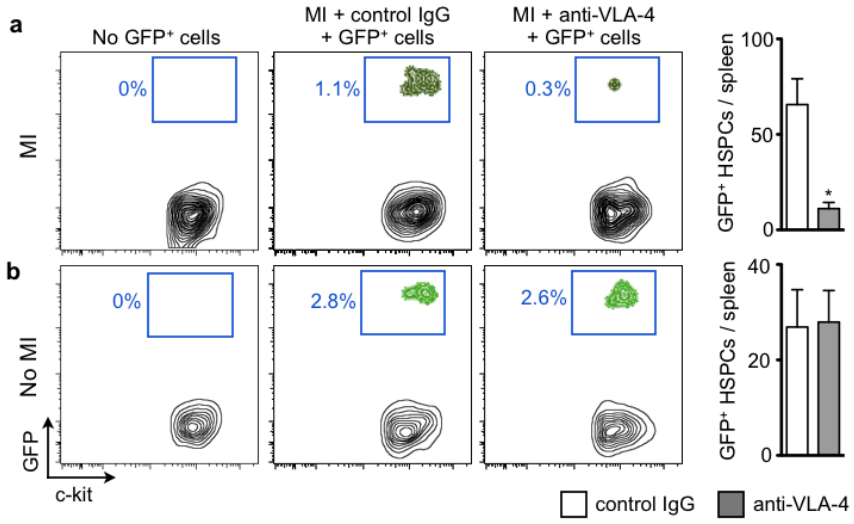


**Supplementary Figure 29: VLA-4 neutralization and splenic engraftment of progenitors after MI and in steady state.**

Flow cytometric enumeration of adoptively transferred GFP$^+$ HSPCs in mice with MI (**a**) or no MI (**b**) treated with either anti-mouse VLA-4 antibody or control IgG (n = 4 per group). Mice without treatment and cell transfer served as a negative control. Previous work[1] showed no effect of neutralizing VLA-4 on stem cell retention in the spleen after bone marrow transplantation into irradiated recipients, a contrast most likely caused by a different splenic milieu in non-irradiated mice with myocardial infarction. Mean ± s.e.m. * $P < 0.01$ versus control IgG.

## Supplementary Table 1

a

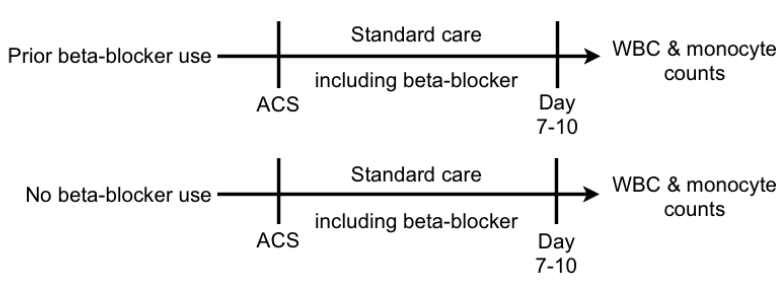


b

**Association between prior beta-blocker use and baseline WBC and monocyte counts**

| | Prior BB use | No BB use | p-value |
|---|---|---|---|
| **WBC count** | N=989 | N=3100 | |
| Median | 8.2 | 9.0 | <0.0001 |
| Interquartile range | 6.8-10.0 | 7.3-11.0 | |
| | | | |
| **Monocyte count** | N=874 | N=2752 | |
| Median | 0.61 | 0.65 | <0.01 |
| Interquartile range | 0.48-0.80 | 0.49-0.84 | |

BB: beta-blocker; WBC: white blood cell

c

**Linear regression analysis of patients with prior beta-blocker use and WBC and monocyte counts**

| | Number of observations | Correlation coefficient | [95% CI] | p-value |
|---|---|---|---|---|
| **Univariate analysis** | | | | |
| WBC count | 4089 | -0.081 | [-0.103, -0.059] | <0.001 |
| Monocyte count | 3626 | -0.017 | [-0.033, -0.001] | 0.038 |
| **Multivariate analysis*** | | | | |
| WBC count | 3485 | -0.063 | [-0.087, -0.039] | <0.001 |
| Monocyte count | 3090 | -0.017 | [-0.035, 0.001] | 0.067 |

* Adjusted for age, gender, time from symptom onset to randomization, history of CHF, and creatinine clearance

**Supplementary Table 1: β-adrenergic blocker administration associates with reduction in white blood cell and monocyte counts in patients after an acute coronary syndrome.**
**a,** Schematic representation of study design and retrospective analysis. **b,** Association between prior beta-blocker use and white blood cell and monocyte counts (expressed as $10^9$/l) in patients 7 to 10 days after an acute coronary syndrome. **c,** Linear regression analysis of patients with prior beta-blocker use and log white blood cell and log monocyte counts. Multivariate analysis was adjusted for age, gender, time from symptom onset to randomization, history of chronic heart failure, and creatinine clearance.

## SUPPLEMENTARY METHODS

**Animal models.** C57BL/6J, B6.SJL-*Ptprc*$^{a}$ *Pepc*$^{b}$/BoyJ, C57BL/6-Tg(UBC-GFP)30Scha/J and B6.129P2-*Apoe*$^{tm1Unc}$/J mice were purchased from Jackson Laboratory. ApoE$^{-/-}$ mice were on C57BL/6 background, but lacked apolipoprotein E that is essential for the normal catabolism of triglyceride-rich lipoprotein constituents. ApoE$^{-/-}$ mice were fed a high-cholesterol diet (Harlan Teklad, 0.2% total cholesterol). Myocardial infarction (MI) was performed on apoE$^{-/-}$ mice when they were on the high-cholesterol diet for 10 weeks. The group assignment (MI versus no MI) was random. Tissues collected from the mice were analyzed at either 1, 3, 6, or 12 weeks after MI. Tissues from C57BL/6 mice were collected and analyzed at either 6, 48, or 96 hours after MI.

To induce MI[2], mice were intubated and ventilated with 2% isoflurane supplemented with oxygen. Thoracotomy was performed in the fourth left intercostal space. The left coronary artery was identified and permanently ligated with a monofilament nylon 8-0 suture. The thorax was closed with glue.

Intraluminal middle cerebral artery occlusion (MCAO) was performed to induce transient cerebral ischemia causing stroke[3]. A middle neck incision was made. Then the left common carotid artery was carefully dissected without harming the vagal nerve and ligated with a 6-0 suture. The left external carotid artery was also ligated. The left internal carotid artery and the left pterygopalatine artery were clipped using microvascular clips. A monofilament (Doccol Corporation) made of 8.0 nylon was introduced through the left common carotid artery before its bifurcation. The clipped arteries were opened and the monofilament blocked the middle cerebral artery. After 45 minutes, the monofilament was withdrawn and the skin was closed with suture. Regional cerebral blood flow was measured with Laser Doppler (Instruments Inc.) to confirm occlusion and reperfusion. Rectal temperature was maintained at 37.5 ± 0.5$^{o}$C during surgery.

**Treatment with 6-hydroxydopamine hydrobromide (6-OHDA).** 6-OHDA (Sigma-Aldrich) was injected i.p at a dose of 250 mg kg$^{-1}$ body weight in a final volume of 200 µl one day before MI in C57/BL6 mice. ApoE$^{-/-}$ mice were treated with the drug once a week for three weeks starting one day before inducing MI.

**Treatment with adrenergic $\beta_3$ receptor antagonist.** SR 59230A, a selective antagonist for adrenergic $\beta_3$ receptor was obtained from Sigma-Aldrich. Mice were injected with the drug intraperitoneally twice daily at a dose of 5 mg kg$^{-1}$ body weight in a final volume of 100 µl in PBS[4]. ApoE$^{-/-}$ mice were treated with the drug for three weeks.

**In vivo neutralization assays.** C57BL/6 mice were injected i.v with 300 µg of either anti-mouse SCF antibody (R&D systems) or control goat IgG (R&D systems) diluted in 300 µl of PBS on the day before and 2 days after MI. For VLA-4 neutralization, mice were injected i.v. with 200 µg of either anti-mouse VLA-4 (BioXCell) or control rat IgG2b (BioXCell) 2 days after MI. About 400,000 lineage$^{-}$ c-kit$^{+}$ cells sorted from GFP$^{+}$ mice were adoptively transferred i.v. on the day of MI.

**Organ and tissue processing.** Blood was drawn via cardiac puncture in 50mM EDTA (Sigma-Aldrich), which was followed by red blood cell lysis with 1x RBC lysis buffer (BioLegend). Spleen and bone marrow were processed in PBS with 0.5% bovine serum albumin and 1% fetal bovine serum (FACS buffer). Aorta was excised under a microscope and minced in digestion mixture containing 450 U/ml collagenase I, 125 U/ml collagenase XI, 60 U/ml DNase I, and 60 U/ml hyaluronidase (Sigma-Aldrich) and incubated at 37$^{o}$ C at 750 rpm for 1 hour[5]. After this the digestion reaction was stopped with 10 ml FACS buffer.

**Flow cytometry.** The processed single cell suspensions (300 µl) were taken in 5 ml falcon tubes (BD Bioscience) for staining with fluorochrome-labelled antibodies against mouse hematopoietic lineage markers[2,5]. For monocyte staining, a Phycoerythrin (PE) anti-mouse lineage antibody cocktail containing antibodies directed against CD90 (clone 53-2.1), B220 (clone RA3-6B2), CD49b (clone DX5), NK1.1 (clone PK136), Ly-6G (clone 1A8) and Ter-119 (clone TER-119) was used. Monocytes were then stained with anti-mouse CD11b (clone M1/70), CD11c (clone HL3), F4/80 (clone BM8) and Ly6C (clone AL-21). Monocytes were identified as (CD90/B220/CD49b/NK1.1/Ly-6G/Ter119)$^{low}$, CD11b$^{high}$, F4/80$^{low}$, CD11c$^{neg/low}$, Ly-6C$^{high/low}$.

For progenitor cell staining, in addition to the antibodies mentioned above, we also used PE-conjugated antibodies directed against CD11b (clone M1/70), CD11c (clone N418), and IL7Rα (clone A7R34) in the lineage cocktail. The cells were then stained with antibodies against c-kit (clone 2B8), Sca-1 (clone D7), CD16/32 (clone 2.4G2), CD34 (clone RAM34), and CD115 (clone AFS98). Hematopoietic stem and progenitors cells (HSPCs) were identified as lineage (CD90/B220/CD49b/NK1.1/Ly-6G/Ter119/CD11b/CD11c/IL7Rα)$^{low}$ c-kit$^{high}$ Sca-1$^{high}$. Granulocyte and macrophage progenitors (GMPs) were identified as lineage$^{low}$ c-kit$^{high}$ Sca-1$^{low}$ CD115$^{low}$ CD16/32$^{high}$ CD34$^{high}$. Macrophage dendritic cell progenitors (MDPs) were identified as lineage$^{low}$ c-kit$^{high}$ Sca-1$^{low}$ CD115$^{high}$ CD16/32$^{high}$ CD34$^{high}$. For in vivo BrdU proliferation assays, the mice were injected intraperitoneally with 1 mg of BrdU (BD Pharmingen) in 100 µl PBS. Tissues were collected the next day and intracellular BrdU staining was performed using BrdU Flow Kits (BD Pharmingen).

**Cell sorting.** In adoptive transfer experiments, donor cells were obtained by crushing all long bones (femur, tibia, fibula, humerus) and spines using a pestle and a mortar in FACS buffer. The cells were passed through 40 µm filters. Red blood cells were lysed and cells were stained with phycoerythrin (PE)-conjugated lineage antibodies as mentioned above, followed by incubation with anti-PE microbeads (Miltenyi). The unconjugated cells, which were enriched for progenitor cells, were separated using magnetic columns according to the manufacturer's instruction. For progenitor cell isolation, the enriched cells were stained with antibodies discussed above and sorted using a FACSAria IIu cell sorter (BD Biosciences) prior to their intravenous adoptive transfer. Depending on the specific experiment, each recipient mouse was injected with 400,000 GFP$^{+}$ donor lineage$^{-}$ c-kit$^{+}$ progenitor cells or 100,000 GMPs 6 hours after induction of myocardial infarction. For photoconversion experiments, each recipient was injected with 25,000 to 40,000 Flk-2$^{-}$ HSPCs 4 days before MI. Tissues from recipient mice were collected and

analyzed by flow cytometry 4 days after MI. For isolation of Ly-6C$^{high}$ monocytes from the aorta 3 weeks after MI, single cell suspensions were prepared from the aorta as discussed above. Monocyte staining was performed using the antibodies mentioned above. Ly-6C$^{high}$ monocytes were sorted using a FACSAria IIu cell sorter (BD Biosciences).

**Quantitative RT-PCR.** Messenger RNA (mRNA) was extracted from aortic roots and bone marrow using a RNeasy Micro Kit (Qiagen) using manufacturer's protocol. One microgram of mRNA was used to generate complimentary DNA (cDNA) using a high capacity RNA to cDNA kit (Applied Biosystems). Taqman gene expression assays (Applied Biosystems) were used to quantify target genes. Variability in loading different amount of cDNA was normalized using Gapdh, a house keeping gene.

**PCR.** RNA was extracted from Ly-6C$^{high}$ monocytes sorted from the aortas of 3 mice per group using a RNeasy Micro Kit (Qiagen). Exactly 3,000 monocytes were isolated from atherosclerotic plaque using a tissue harvesting and antibody incubation protocols as described under Cell sorting using a FACSAria III cell sorter. QuantiTect Whole Transcriptome kit (Qiagen) was used to prepare cDNA from total RNA and make enough cDNA for the array by linear amplification according to manufacturer's protocol. In short, reverse transcription reaction was performed at 37$^{o}$ C for 30 minutes to generate cDNA from mRNA. The reaction was stopped by an incubation at 95$^{o}$C for 5 minutes. The synthesized cDNA was ligated using a ligation mix at 22$^{o}$C for 2 hours. Finally, whole transcriptome amplification was performed at 30$^{o}$C for 8 hours to generate cDNA. Three sets of primers were designed using online tools of Integrated DNA Technologies (http://www.idtdna.com/Scitools/Applications/RealTimePCR/). The specificity of the primers was validated using Sybr Green dissociation curves. Sybr Green-based quantitative PCR was performed using a 7300 real-time PCR system (Applied Biosystems). All samples were run in triplicates. Raw Ct values were normalized according to expression of Ly-6C and a heat map of relative normalized expression (Δct) data was generated using Cluster3 and Java Treeview applying an uncentered correlation metric for hierarchical clustering.

For comparison of Ly-6C$^{high}$ monocyte phenotype in bone marrow versus spleen, cells were isolated as described under cell sorting using a FACSAria IIu cell sorter from 6 mice per group, on day 4 after coronary ligation. Monocyte staining was performed as discussed in the 'Flow Cytometry' section after depleting the lineage$^{+}$ cells. Exactly 100,000 Ly-6C$^{high}$ monocytes were sorted from each organ per mouse and analyzed by PCR. cDNA was prepared from the total RNA extracted from the cells. Linear amplification of cDNA and Sybr Green-based quantitative PCR were performed for 32 genes. Raw Ct values were normalized to expression of Ly-6C, which was similar in both populations. A heat map of ΔCt values after mean centering for each gene was generated using the R environment for statistical computing. P-values were calculated using a two-sided t-test and Bonferroni corrected for multiple testing.

**Intravital microscopy.** CD45.1$^{+}$ wild-type C57BL/6 mice were Flk-2$^{-}$ HSPC donors when recipients were CD45.2$^{+}$ C57BL/6 mice. After cell sorting, 1–1.5 x 10$^{6}$ cells per ml Flk-2$^{-}$ HSPCs were stained with 5 μM DiD in PBS without serum for 10 min at 37$^{o}$ C, washed once in PBS,

and injected into the tail vein of recipient mice. Each imaged $CD45.2^+$ mouse received the same number of DiD-labelled $CD45.1^+$ HSPCs (25,000 to 40,000 according to different experiments). Mice were anesthetized and prepared for in vivo imaging as previously described[6]. Immediately before imaging, 25 µl of non-targeted Qdot 800 (Invitrogen) diluted in 100 µl sterile PBS was injected i.v. to allow vasculature visualization. The mouse was held in a heated tube mounted on a precision 3 axis motorized stage (Suter MP385). Cells within the skull bone marrow cavity were imaged with 635 nm laser illumination using a custom-built confocal two-photon hybrid microscope specifically designed for live animal imaging as described previously[6]. At the start of each imaging session, large areas of the skull bone surface were surveyed using video rate second harmonic microscopy generated by collagen in the bone to identify the major anatomical landmarks such as sagittal and coronal sutures. The locations of HSPCs within bone-marrow cavities were identified and their coordinates recorded relative to the intersection of the sagittal and coronal sutures. Data were acquired as Z-stacks at 5 µm steps containing 3 separate channels: bone (assigned to the blue channel), vasculature (assigned to the red channel) and transplanted HSPCs (DiD signal, assigned to the white channel). Image processing was performed using Image J software. After in vivo imaging, the scalp was closed and post-operative care was provided.

**Photoconversion experiments**. Flk-$2^-$ HSPCs were harvested from the bone marrow (long bones, spine) of 30 $CD45.2^+$ donor mice per one $CD45.1^+$ recipient. Cells were isolated as described under cell sorting and then labeled with the near IR fluorescent, lipophilic carbocyanine $DilC_{18}(7)$ (DiR, Invitrogen) and injected i.v. into CD45.1 recipients. Four days after adoptive transfer, these cells were located in the skull by intravital microscopy as described above and then photoconverted in vivo by illuminating for 20 seconds with a 750 nm laser (≤50 mW on the sample), changing the fluorescence of the dye from 780 nm to 670 nm. Immediately thereafter, converted cells were imaged by IVM in the bone marrow after excitation with the 635 nm laser to ensure that the color of the cells had changed. In one control mouse cells were not photoconverted. Two mice underwent coronary ligation after photoconversion, whereas two control mice did not. Four days after photoconversion, cells were harvested from the spleen. A splenic cell suspension was produced from the entire organ, which was lineage depleted with magnetic beads, stained for DAPI and FITC anti-mouse CD45.2 (Clone 104; BD Pharmingen), mounted on slides and finally imaged ex vivo as described previously[6].

**Fluorescence Molecular Tomography-Computed Tomography (FMT/CT).** FMT/CT was performed to investigate how MI changes protease activity of atherosclerotic plaques of $apoE^{-/-}$ mice[7]. Before inducing MI and then again three weeks after the MI, FMT-CT imaging (680/700 nm excitation/ emission) was performed to investigate magnitude of inflammation. $ApoE^{-/-}$ mice without MI were used to as control. Five nmol of a pan-cathepsin protease sensor (Prosense-680) were injected i.v. 24 hours before imaging. A quantitative 3D dataset in which fluorescence per voxel was expressed in nM was reconstructed. FMT was followed by CT (Inveon PET-CT, Siemens) to identify anatomic regions[8]. Contrast-enhanced high resolution CT localized the aortic root, a prominent site of plaque formation in $apoE^{-/-}$ mice. This anatomical information guided the placement of the volume of interest in the quantitative protease activity map

concomitantly obtained by hybrid FMT. An imaging cartridge containing the anesthetized mouse was placed into a custom machined plexiglas holder that supplies isoflurane during imaging. The CT x-ray source with an exposure time of 370-400 ms was operated at 80 kVp and 500 μA. During CT, isovue-370 was infused continuously at 55 μL/min through a tail vein catheter. The CT reconstruction protocol performed bilinear interpolation, used a Shepp-Logan filter, and scaled pixels to Hounsfield units. Image fusion relied on fiducial markers and used Osirix software (The Osirix Foundation, Geneva).

**Fluorescence reflectance imaging (FRI).** The mice were sacrificed after the second FMT-CT. Aortas were excised under a microscope and imaged using a planar fluorescent reflectance imaging system (OV-110, Olympus) with an excitation wavelength 680 nm. Light and near infrared fluorescence (NRIF) images were obtained with respective exposure times between 75 msec and 60 seconds.

**Histology.** Aortic roots were collected, embedded in O.C.T. compound (Sakura Finetek), and flash-frozen in a 2-methylbutane bath with dry ice. Sections of 5 μm thickness were stained with anti-CD11b antibody (clone M1/70, BD Biosciences) followed by a biotinylated anti-rat secondary antibody (Vector Laboratories, Inc.) VECTA STAIN ABC kit (Vector Laboratories, Inc.) and AEC substrate (DakoCytomation) were used for color development. Cells with CD11b staining were quantified using IPLab (version 3.9.3; Scanalytics, Inc.). For fibrous cap and necrotic core analysis, aortic roots were stained with Trichrome stain (MASSON) (Sigma-Adlrich). Fibrous cap thickness and necrotic core were quantified using Masson stained aortic root sections scanned with NanoZoomer 2.0-RS (Hamamatsu) in 40x magnification as previously described[9]. Briefly, for fibrous cap thickness, 5 measurements of the thinnest fibrous caps per plaque were averaged. Necrotic cores were analyzed by measuring total acellular areas within each plaque[9]. Toluidine Blue staining was carried out to detect mast cells. After aortic roots sections were fixed with 10% formalin solution, the sections were stained in Toluidine blue working solution (1.0g of Toluidine Blue O (Sigma-Adlrich) in 100mL of 70% alcohol and 1% Sodium chloride in distilled water adjusted pH to 2.3), washed in distilled water, and dehydrated quickly prior to clearing in xylene and cover slipping. Femurs were harvested, fixed in 4% paraformaldehyde for 3 hours, and immersed in 0.375M EDTA in PBS for 10 days for decalcification prior to paraffin embedding. The paraffin-embedded sections were deparaffinized, rehydrated, and stained with anti-tyrosine hydroxylase antibody (Millipore). The slides were scanned with a NanoZoomer 2.0-RS (Hamamatsu) at 40x magnification and quantified using IPLab (version 3.9.3; Scanalytics, Inc.). For immunofluorescence microscopy, frozen spleen sections were stained with SCF (clone H-189, Santa Cruz Biotechnology, Inc.), nestin (clone 7A3, abcam), CD31 (clone MEC13.3, BD Biosciences), and CD31: Alexa Fluor 488 (clone ER-MP12, AbD Serotec). Alexa Fluor 488 chicken anti-rabbit IgG (Molecular Probes) and Alexa Fluor 594 donkey anti-rat IgG (Jackson ImmunoResearch Laboratories, Inc.) were used as secondary antibodies. The slides were cover slipped using a mounting medium with DAPI (Vector Laboratories, Inc.) to identify nuclei. Images were observed and captured using Nikon Eclipse 80i with a Cascade Model 512 B camera (Roper Scientific) with a Cy5.5 filter cube (HQ650/45x EX, dichroic Q680LP BS, and emission filter HQ710/50m EM), Y-2E/C (D560/40x

EX, dichroic 595DCLP BS, and emission filter D630/60m EM), GFP/FITC (HQ480/40x EX, dichroic Q505LP BS, and emission filter HQ535/50m EM), and UV (D365/10x EX, dichroic 380DCLP BS, and emission filter E400LPv2 EM, Chroma Technology Corp.)

**Human spleen tissue collection.** Autopsy samples of spleen tissue was collected from 29 patients who died hours to days after acute myocardial infarction (mean age 65 ± 3, 21 men) and 13 control trauma cases (42 ± 6 years, 9 men) at Heidelberg University, Germany. Spleen tissue was also stained in additional autopsy studies at the University of Amsterdam, The Netherlands, where the use of patient material after completion for the diagnostic process is part of the patient contract in the VUmc hospital. The study was conducted in accordance with the Declaration of Helsinki, and the study protocol was approved by the institutional medical ethics committee. Deparaffinized and rehydrated sections were incubated with 10% goat serum, followed by incubation with rabbit anti-c-kit (clone YR145, 1:25, Cellmarque, Rocklin, CA, USA) and mouse anti-Ki-67 (clone MIB-1, 1:150, Dako, Copenhagen, Denmark). Sections were then incubated with goat anti-rabbit IgG Alexa Fluor 555 and goat anti-mouse IgG Alexa Fluor 488 (each 1:200; Molecular Probes, Leiden, The Netherlands), and counterstained with Hoechst 33342. After fluorescence labeling, the slides were immersed for 30 min in 70% ethanol supplemented with 0.1% Sudan Black B (Merck, Darmstadt, Germany). Stained sections were examined under Leica DM6000 microscope (Leica Microsystems, Heidelberg, Germany). Immunoenzyme stainings of c-kit and Ki-67-clones were performed on 2-µm paraffin sections of formalin-fixed tissues using standard avidin-biotin anti–alkaline phosphatase techniques (Vectastain; Vector Laboratories). Antigen retrieval was achieved by steam-cooking the slides in 10 mM citrate buffer (pH 6.1; Dako) for 30 min. A solution of 10% Earle's balanced salt solution (EBSS, Sigma-Aldrich) supplemented with 1% Hepes, 0.2% BSA, and 0.1% saponin (all from Sigma-Aldrich), pH 7.4, was used as a washing and permeabilization buffer. Primary Ab dilutions also were prepared in this buffer with 4% γ-venin (Behring) added and incubated overnight at 4 °C. Biotinylated sheep anti-mouse IgG was applied as a secondary reagent for 30 min at room temperature. Naphthol AS-biphosphate (Sigma-Aldrich) with New Fuchsin (Merck) was used as the substrate for alkaline phosphatase.

**Blood cholesterol and HDL measurement.** Using a cardiac puncture, blood was drawn from apoE$^{-/-}$ mice and collected in eppendorf tubes without anti-coagulant. Blood was kept at room temperature for an hour followed by a spin at $4^0$ C for 20 minutes. Serum was carefully collected without red blood cell contamination and stored at $-20^0$ C. Total cholesterol and HDL were measured using an enzymatic colorimetric assay (Cholesterol E, Wako Diagnostics) according to manufacturer's instructions.

**Analysis of white blood cell and monocyte counts in patients.**
The Pravastatin or Atorvastatin Evaluation and Infection Therapy – Thrombolysis in Myocardial Infarction 22 (PROVE IT-TIMI 22) trial was a multicenter, randomized controlled trial of intensive versus standard lipid lowering therapy in patients hospitalized for an acute coronary syndrome within the previous 7-10 days[10]. The current analysis focused on comparing white blood cell and monocyte counts on day 7-10 after acute coronary syndrome in patients with and

without beta-blocker use prior to enrollment, as defined by an interview with the patient and a review of medical records by trained researchers. White blood cell and monocyte counts were assessed in the laboratories at local enrolling institution and recorded on a case report form. Descriptive statistics were expressed as median with interquartile range for continuous variables. Differences in white blood cell and monocyte counts between patients with prior beta-blocker use versus those without were assessed by the Wilcoxon rank-sum test. Univariate linear regression analysis was performed to evaluate the relationship between prior beta-blocker use and white blood cell or monocyte counts (both log transformed). Multivariate linear regression analysis was also performed after adjusting for potential confounders: age, gender, time from symptom onset to randomization, history of congestive heart failure, and creatinine clearance.

**Statistics.** Results are expressed as mean ± standard error of mean. Data was tested for normality using the D'Agostino-Pearson normality test, and for equality of variances using the Bartlett's test. If normality and equality of variances were not rejected at 0.05 significance level, the group means were compared using a t-test (for 2 groups) and ANOVA, followed by Bonferroni post tests (for > 2 groups). P values of $<0.05$ indicate statistical significance. For non-normally distributed data and data with unequal variances, we applied nonparametric tests, such as Mann-Whitney U.

**SUPPLEMENTARY REFERENCES**


1. Katayama, Y. et al. PSGL-1 participates in E-selectin-mediated progenitor homing to bone marrow: evidence for cooperation between E-selectin ligands and alpha4 integrin. *Blood* **102**, 2060-2067 (2003).
2. Nahrendorf, M. et al. The healing myocardium sequentially mobilizes two monocyte subsets with divergent and complementary functions. *J Exp Med* **204**, 3037-3047 (2007).
3. Qiu, J. et al. Early release of HMGB-1 from neurons after the onset of brain ischemia. *J Cereb Blood Flow Metab* **28**, 927-938 (2008).
4. Mendez-Ferrer, S., Lucas, D., Battista, M. & Frenette, P. S. Haematopoietic stem cell release is regulated by circadian oscillations. *Nature* **452**, 442-447 (2008).
5. Swirski, F. K. et al. Ly-6Chi monocytes dominate hypercholesterolemia-associated monocytosis and give rise to macrophages in atheromata. *J Clin Invest* **117**, 195-205 (2007).
6. Lo Celso, C., Lin, C. P. & Scadden, D. T. In vivo imaging of transplanted hematopoietic stem and progenitor cells in mouse calvarium bone marrow. *Nat Protoc* **6**, 1-14 (2011).
7. Nahrendorf, M. et al. Hybrid in vivo FMT-CT imaging of protease activity in atherosclerosis with customized nanosensors. *Arterioscler Thromb Vasc Biol* **29**, 1444-1451 (2009).
8. Nahrendorf, M. et al. Hybrid PET-optical imaging using targeted probes. *Proc Natl Acad Sci U S A* **107**, 7910-7915 (2010).
9. Seimon, T. A. et al. Macrophage deficiency of p38alpha MAPK promotes apoptosis and plaque necrosis in advanced atherosclerotic lesions in mice. *J Clin Invest* **119**, 886-898 (2009).

10. Cannon, C. P. et al. Intensive versus moderate lipid lowering with statins after acute coronary syndromes. *N Engl J Med* **350**, 1495-1504 (2004).